scientific reports

Check for updates

OPEN

# Identification of high-risk soil erosion areas in the central Yunnan urban agglomeration and the differentiated driving mechanisms compared to the overall agglomeration

Dongling Ma[1,2], Shuangyun Peng[1,2]✉, Zhiqiang Lin[1,2], Bangmei Huang[3], Ziyi Zhu[1,2] & Shuangfu Shi[1,2]

**Revealing the complex driving mechanisms of soil erosion is essential for assessing regional ecological security. Focusing on the Central Yunnan Urban Agglomeration (CYUA), a typical mountainous urban region, this study analyzed the spatiotemporal dynamics of soil erosion from 1990 to 2020 using the RUSLE model and the Improved Stability Mapping (STD) method, identifying high-risk soil erosion areas. Additionally, it applied the OPGD and MGWR models to reveal differentiated driving mechanisms of soil erosion across the urban agglomeration and in high-risk zones. The results indicated that (1) over the past three decades, approximately 27.56% of the CYUA experienced soil erosion, with moderate and high-intensity erosion accounting for 7.04% and 3.83%, respectively. Soil erosion increased continuously from 1990 to 2000 but showed significant improvement after 2000. (2) High-risk areas identified using the improved STD method were primarily distributed along riverbanks, which are highly sensitive to external disturbances. (3) Slope and vegetation were the key factors affecting the overall soil erosion pattern in the urban agglomeration, while rainfall and vegetation were the dominant influencing factors in high-risk areas, where spatial heterogeneity of driving factors was lower than in the general region. (4) Vegetation cover had a significant mitigating effect on soil erosion, making increased vegetation coverage an effective strategy for soil and water conservation. This study provides new insights for soil erosion risk assessment and offers a scientific basis for regional soil erosion control and ecological restoration.**

**Keywords** Spatiotemporal dynamics, High erosion risk areas, Driving mechanisms, Differentiation analysis, Improved stability mapping (STD) method

Soil, hailed as the lifeline of humanity[1], bears a crucial role in food production[2], water resource conservation[3], and ecosystem support[4], serving as the cornerstone of high-quality human life and sustainable development. However, global environmental changes have intensified soil erosion, impacting land productivity[5] and ecological balance[6], threatening food security[7], and leading to alterations in the content and composition of elements such as carbon and nitrogen in the soil[8], which in turn affect global biogeochemical cycles and climate[9]. Therefore, accurately understanding the spatiotemporal dynamics of soil erosion and its driving mechanisms is essential for formulating effective soil erosion prevention strategies and promoting sustainable development at both regional and global levels[10,11].

Previous studies have primarily focused on assessing overall soil erosion and analyzing driving factors at a regional level[12,13], while detailed identification of high erosion risk areas and their differentiated driving mechanisms has received comparatively less attention. These studies often emphasize macro-level analysis,

[1]Faculty of Geography, Yunnan Normal University, Kunming 650500, China. [2]GIS Technology Engineering Research Centre for West-China Resources and Environment of Educational Ministry, Kunming 650500, China. [3]Kunming No. 10 High School, Kunming 650011, China. ✉email: frankmei@126.com

overlooking the dynamic characteristics of localized high-risk areas, which hinders the provision of effective support for precise prevention strategies. In recent years, methods for identifying soil erosion risk areas have continuously evolved. However, traditional spatiotemporal analysis methods typically rely on average soil erosion rates at a single time point or a singular sensitivity index[14] to identify high-risk areas, making it difficult to capture the dynamic changes and complexities of the soil erosion process across different time scales[15]. Consequently, traditional methods for identifying high erosion risk areas have limitations in addressing multi-temporal variations and the nonlinear development of soil erosion, resulting in insufficient identification accuracy. The improved Stability Mapping (STD) method offers a new perspective to address this issue. This method comprehensively considers the similarity, turnover rate, and diversity of soil erosion, enabling the refined identification of different types of change trajectories, particularly significant fluctuations in high-risk areas. Compared to traditional methods, the improved STD approach not only overcomes the limitations of single-phase analysis but also captures the complex dynamic changes of soil erosion across different time scales, effectively identifying and quantifying spatial dependencies, and accurately capturing change trends and key areas[16]. Applying this method contributes to a deeper understanding of the dynamic changes in soil erosion and provides a scientific basis for formulating more targeted soil erosion prevention and control measures, thereby promoting sustainable regional management.

Changes in soil erosion constitute a complex and multifaceted process, resulting from the combined impacts of natural phenomena and human activities[17]. Land use/cover change and climate change are generally acknowledged as the primary and dynamic forces driving soil erosion[18–20]. Although these factors are universal, the dominant drivers of soil erosion vary significantly across regions. For example, alterations in water and soil loss in the lower Yellow River area primarily stem from differences in elevation and land use types[21]; conversely, rainfall patterns and land use changes dictate soil erosion on the island of Crete in the Mediterranean region[20]; and in the karst areas of Southwest China, vegetation types and rainfall conditions significantly impact water and soil loss[22]. Therefore, the principal drivers of soil erosion differ by region, making it crucial to explore the driving factors in different areas. However, the linkage between these driving forces and soil erosion is not a straightforward linear relationship but rather the consequence of multiple factors operating in conjunction[23]. Consequently, delving into the comprehensive driving factors behind soil erosion has become an essential research topic.

Current models for attributing driving factors can be divided into non-spatial models (such as multiple regression[24], redundancy analysis[25], ordinary least squares[26], etc.) and spatial models (such as Geographical Detector[27], geographically weighted regression, etc.)[28]. Non-spatial models overlook the impact of geographical location. In contrast, spatial models incorporate spatial position and its dependencies, revealing the heterogeneity of driving factors across varied geographic areas, offering a fresh perspective for understanding intricate geographical phenomena[29]. Spatial models can quantitatively analyze the spatial diversity of causal elements; therefore, research on spatial models in investigating the causal elements of changes in soil erosion is increasing. However, challenges remain: the spatial data discretization of traditional Geographical Detector introduces subjectivity and randomness[30], increasing analytical uncertainty; and most studies do not fully consider the scale characteristics of driving factors[31]. Addressing these challenges, this study integrates LASSO regression, Optimal Parameter Geographical Detector (OPGD), and Multiscale Geographically Weighted Regression (MGWR) methods. The LASSO regression method can effectively solve the multicollinearity problem, avoiding overfitting and helping to build more reliable models[32]. OPGD reduces subjectivity and randomness by optimizing the data discretization process and parameter selection, improving the accuracy and reliability of spatial analysis[33]. Simultaneously, the MGWR method considers heterogeneity at different spatial scales, allowing for a more accurate capture and understanding of the influence of underlying determinants at various geographical scales[34]. The combined application of these three methods not only enhances the ability to explain the spatial interdependence of driving forces but also reveals the distribution characteristics and intensity of influence of soil erosion determinants at diverse geographic levels, thereby offering specific strategies for soil erosion prevention and control.

This study focuses on the Central Yunnan Urban Agglomeration (CYUA), a representative mountainous urban area in southwest China characterized by significant elevation variations, complex geological structures, and variable climatic conditions, leading to serious soil erosion issues. To this end, this study employs an improved RUSLE model for a quantitative assessment of soil erosion from 1990 to 2020 and uses the improved STD method to identify high erosion risk areas. Based on this, the study employs the Optimal Parameter Geographical Detector (OPGD) and Multiscale Geographically Weighted Regression (MGWR) models to analyze the differentiated driving mechanisms of soil erosion in the urban agglomeration as a whole and in high erosion risk areas, aiming to reveal the dominant factors of soil erosion in different regions and their spatial characteristics. The results will contribute to a deeper understanding of the spatiotemporal evolution patterns and driving mechanisms of soil erosion in the CYUA, providing scientific references for regional soil conservation and ecological environment.

## Materials and methods

### Study area

The Central Yunnan Urban Agglomeration (CYUA) is situated in the southern part of the Qinghai-Tibet Plateau (100°45 ×104°48′E,23°20 ×27°02′N), encompassing Kunming, Qujing, Yuxi, Chuxiong, and the northern portion of Honghe, which includes 7 cities and counties (Shiping, Jianshui, Kaiyuan, Luxi, Mile, Gejiu, and Mengzi), totaling 49 counties, cities, and districts(Fig. 1). Rainfall and dry periods within the urban agglomeration display significant disparities, with an average yearly rainfall of 950 mm, mainly occurring between June and August, making up approximately 60% of the annual precipitation. The terrain of the urban agglomeration is complex, with mountain ranges extending from northwest to southeast, higher in the north and lower in the

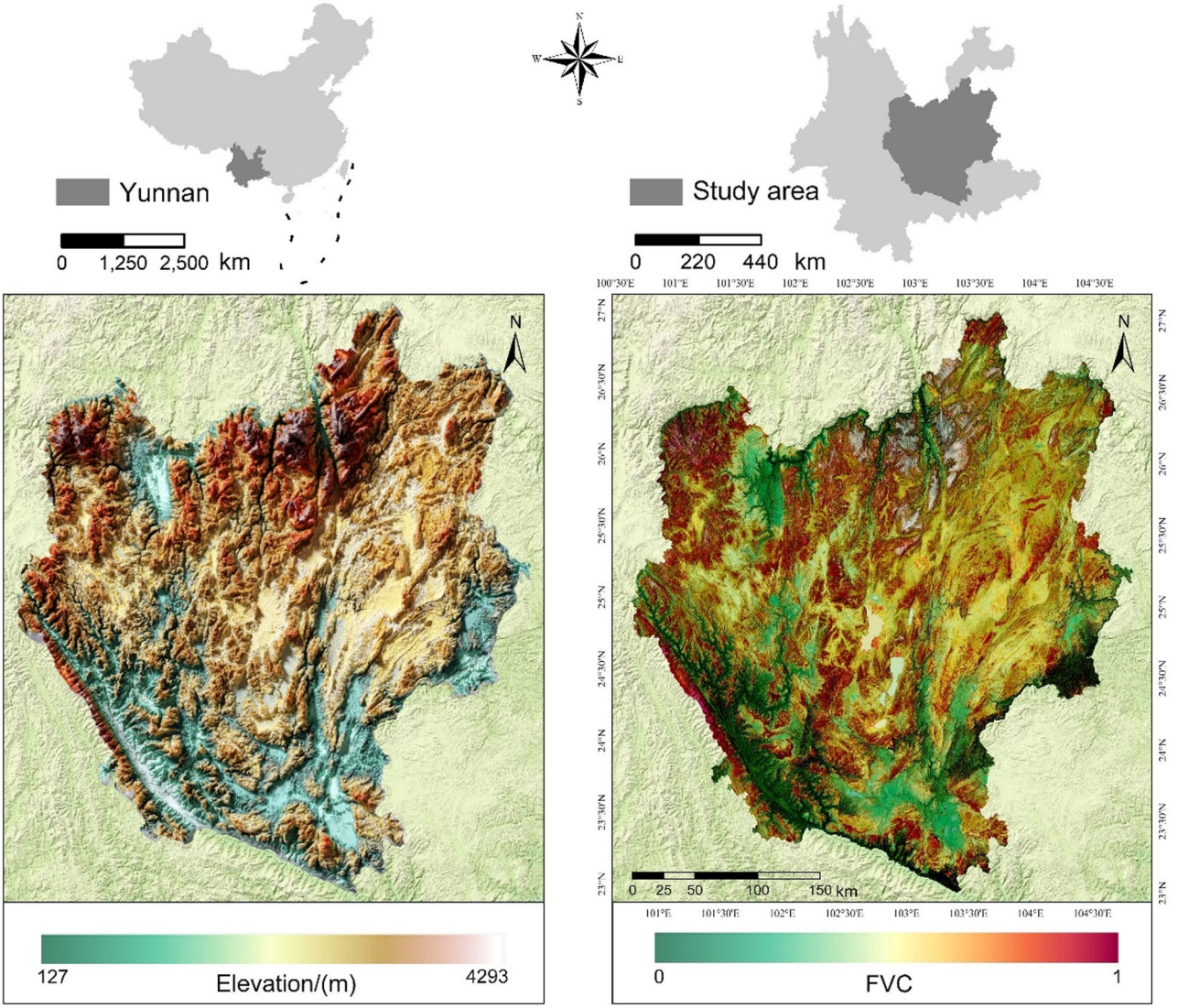


**Fig. 1**. Study area. Figure 1 was generated though the ArcGIS 10.5 software (http://www.esri.com).

south, spanning altitudes from 127 to 4293 m above sea level, showcasing high peaks, deep ravines, and steep inclines. Slopes vary from 0° to 88°, with an average gradient of 15.7°. The region has a considerable amount of arable land and is the most advanced agricultural area in Yunnan Province, hosting the densest population and urban distribution. The combination of complex terrain, intense seasonal rainfall, and intensive land use has led to severe soil erosion in the region.

## Data sources

This study selected the period from 1990 to 2020, aiming to reveal the differentiated driving mechanisms of soil erosion between the urban agglomeration as a whole and high-risk areas. To ensure consistency and comparability of the data, the spatial coordinate system used in this paper is WGS_1984_UTM_zone_48 N, and all data have been resampled to a spatial resolution of 1 km. Detailed information about the data can be found in Table 1.

## Quantification of soil erosion

The Revised Universal Soil Loss Equation (RUSLE) model stands as the most utilized method for assessing soil erosion impacts. Due to its simplicity in structure, constrained parameters, convenient input, and reliable result have led to its extensive use for predicting and analyzing soil erosion on a global scale[35,36]. In this study, the soil erosion modulus for seven consecutive phases from 1990 to 2020 was calculated using RUSLE model. Refer to Supplementary Material S1 for operating procedures of RUSLE model.

| Data | Relevant information | Resource |
|---|---|---|
| ASTER GDEM V2 | 30 m; grid | Geographic Spatial Data Cloud (http://www.gscloud.cn) |
| Landsat series data | 30 m; grid | |
| Daily rainfall, daily temperature: | 99 meteorological stations around CYUA; text | Resource and Environment Science & Data Centre of the Chinese Academy of Sciences (http://www.resdc.cn) |
| Gross Domestic Product(GDP) | 1 km; grid | |
| Population Density(POP) | | |
| Land use data | 30 m; grid | |
| Soil data (including sand, silt, clay, and organic carbon content) | 1 km; grid | World Soil Database (HWSD) (http://www.fao.org) |
| Land use data | 30 m; grid | Resource and Environment Science & Data Centre of the Chinese Academy of Sciences (http://www.resdc.cn) |

**Table 1**. Data description.

| Level | Slight Erosion | Mild Erosion | Moderate Erosion | Severe Erosion | Extremely Severe Erosion | Violent Erosion |
|---|---|---|---|---|---|---|
| Soil Erosion Modulus | 0 ~ 5 | 5 ~ 25 | 25 ~ 50 | 50 ~ 80 | 80 ~ 150 | > 150 |

**Table 2**. Soil erosion intensity classification standards ($t{\cdot}ha^{-1}{\cdot}y^{-1}$).

## Extracting high erosion risk areas based on the stability mapping method

After obtaining the soil erosion modulus, we refered to the "Classification and Grading Standards for Soil Erosion" (SL190-2007) issued by the Chinese Ministry of Water Resources, merge pixels with the same erosion level, and draw a soil erosion intensity map of the urban agglomeration. Specific classification and grading standards can be seen in Table 2.

Based on this, soil erosion intensity levels of severe erosion and above were classified as a new category named "high-intensity soil erosion". Meanwhile, according to the erosion standards issued by the Chinese Ministry of Water Resources, the range of 0–5 $t{\cdot}ha^{-1}{\cdot}y^{-1}$ was considered as an area with no significant erosion; thus, slight erosion was regarded as an area with no significant erosion. In this study, severe erosion, extremely severe erosion, and violent erosion were classified as high-intensity erosion. Thus, no significant erosion, mild erosion, moderate erosion, and high-intensity erosion were encoded as 1, 2, 3, and 4, respectively.

*Extraction of change maps*

The extraction of soil erosion change maps could be viewed as the extraction of multi-temporal soil erosion spatial unit change maps. Referring to the spatial expression method of land use change proposed by Shi et al.[37],, we extracted the changes of soil erosion at various temporal phases within a continuous time series. The formula is as follows:

$$C = 10^{n-1} * Y_1 + 10^{n-2} * Y_2 +, \ldots, +10^{n-i} * Y_{i-1} +, \ldots, +10^{n-n} * Y_i \quad (1)$$

where, $C$ represents the soil erosion change map of the study area in a continuous time series; $n$ is the number of temporal phases during the study period, and $Yi$ represents the soil erosion change map corresponding to the $i$ th temporal phase.

*Improved stable mapping change trajectory extraction*

To delve deeper into the soil erosion changes at specific locations, we adopted the stability mapping change trajectory analysis technique advocated by Swetnam[38], which includes three indices: Similarity, which captures data regarding the prevalent status of any category at a given location throughout the entire period; Turnover which records the frequency of changes occurring between consecutive years; Diversity identifies the number of any category. By integrating this with the real-world context of soil erosion variations in urban agglomerations, this study proposes a suitable STD judgment method for soil erosion changes in urban agglomeration. Then, using logical rules, these three indices were combined into four categories in the time series: stable, step, periodic, and fluctuating (Table 3).

*Identifying high erosion risk areas*

In analyzing the soil erosion change trajectories of the Central Yunnan Urban Agglomeration (CYUA), we applied the stability mapping method to categorize the change trajectories of different plots into four types: stable, stepwise, cyclical, and fluctuating. Among these, the "fluctuating" trajectory exhibited significant soil erosion changes with high uncertainty and potential risk. Therefore, we regarded fluctuating areas as high-sensitivity zones for soil erosion.

The definition of high-sensitivity areas is based on the intense volatility of soil erosion in these regions and their high responsiveness to external factors (such as climate change, precipitation intensity, vegetation cover, and human activities). Fluctuating areas are generally more susceptible to external environmental changes, leading to soil degradation and exacerbation of erosion, which increases ecological risk and necessitates enhanced

| Turnover | Diversity | Similarity | Primary Class | Secondary Class | Example | Features |
|---|---|---|---|---|---|---|
| 0 | 1 | 7 | Stable | Stable | 1,111,111 | No change |
| 2 | 2 | 6 | | Metastable | 1,111,211 | One-year mutation, the rest unchanged |
| 1 | 2 | 6,5 | Step | Early Change Late Stability | 1,121,111 | Only one change occurs between two types in the first three temporal phases |
| 1 | 2 | 4 | | Mid-term Change | 1,112,111 | Only one change occurs between two types in the middle period |
| 1 | 2 | 6,5,4 | | Early Stability Late Change | 1,111,121 | Only one change occurs between two types in the last three temporal phases |
| 2,3,4 | 2,3,4 | 2,3,4 | Periodic | — | 1,212,121 | Fluctuations with certain regularity |
| — | — | — | Fluctuating | — | 1,243,413 | More frequent changes between categories are related to high turnover rates |

**Table 3**. Logical rules for soil erosion change trajectories STD in the CYUA.

management and protection efforts. In subsequent analyzes, high-sensitivity areas will be the focus of attention, combining their specific driving factors to provide more targeted management and protection measures to effectively control soil erosion, reduce ecological risks, and achieve sustainable regional development.

## Analysis of soil erosion drivers

*LASSO regression for driver factor screening*

Changes in soil erosion are intrinsically linked to both environmental elements and human actions. We initially selected 19 potential driving factors and classified them into five categories: terrain (elevation, slope, aspect, terrain wetness index), land use (pattern (edge density, landscape shape index, patch density, cohesion) and structure (proportion of cropland, woodland, grassland, water area, built-up area, unused land, major land use types)), population (population density), vegetation (vegetation coverage), and climate (temperature and precipitation). Utilizing Matlab software, we employed LASSO regression to analyze 19 possible influencers of soil erosion in the CYUA region. The primary objective of this method is to reduce:

$$min\left\{\sum{}_{i=1}^{k}\left(y-\sum{}_{j-1}^{p}x_{ij}\beta_{j}\right)^{2}+\lambda\ \sum{}_{j-1}^{p}\left|\beta_{j}\right|\right\} \tag{2}$$

Where, $\beta_j$ is obtained by solving the minimization problem described in the equation, $\lambda$ is used to control the regularization strength of the coefficients, and its optimal value will be determined based on the model performance indicators obtained through cross-validation.

We used LASSO regression to conduct biased estimation regression on the 19 driving factors. Subsequently, important predictor variables were screened out, all five categories of driving factors had predictor variables retained, totaling 11 variables, encoded as X1 to X11, and Specific description are presented in Supplementary Material S2.

*Optimal parameter geographical detector*

To effectively identify and quantify the effect of these potential elements on soil erosion, it is urgent to recognize these factors and measure their influence quantitatively. In this study, the soil erosion intensity values at different temporal phases were taken as the response variables, with the 11 screened driving factors as explanatory variables. We used the Optimal Parameter Geographical Detector (OPGD) developed based on R language to analyze driving factors[33]. The OPGD tool utilizes both single-factor and interactive detector functions to determine the effect of individual and combined explanatory variables (X) on the response variables (Y) using the q statistic in Eq. (8) as a measure.

$$\begin{gathered} q=1-\frac{SSW}{SST} \\ SSW=\sum{}_{h=1}^{L}N_{h}\sigma_{h}{}^{2} \\ SST=\sigma^{2} \end{gathered} \tag{3}$$

*Multi-scale geographical weighted regression*

While the Geographical Detector can identify important driving factors influencing soil erosion, it primarily analyzes the influence of each factor from a global statistical perspective, making it difficult to reveal the spatial non-stationarity of driving factor influences, i.e., how the degree of influence varies with geographical location. In contrast, the MGWR method, by estimating the local regression coefficients of each explanatory variable at each geographical location, can effectively quantify the spatial non-stationarity of driving factor influences and intuitively demonstrate the spatial heterogeneity of driving factor influences[39]. Although the Geographical Detector can identify the interactions between different factors, its results are still global and cannot reveal the specific spatial manifestations of these interactions. Furthermore, MGWR can handle the characteristic that different explanatory variables may have different spatial scales of influence, which is not achievable with the Geographical Detector.

Thus, it becomes increasingly essential to understand how this phenomenon can be observed on a local scale while incorporating more granular spatial details. To capture the spatial heterogeneity of the relationships between response and explanatory variables, and considering that different variables may operate at different spatial scales, we employed the Multiscale Geographically Weighted Regression (MGWR) method. This approach is particularly effective as it accounts for the varied spatial scales inherent to different variables within

geographical processes[40]. The deployment and computation of the MGWR model follow a structured modeling process, as detailed by Fotheringham et al.[39].

$$Y_i = \sum {}_{j=1}^{p} \beta_{bwj}(u_i, v_i) X_{ij} + \epsilon_i \quad (4)$$

Where, $Y_i$ represents soil erosion, $X_{ij}$ represents the $j$th variable affecting soil erosion of the $i$th sample, $b_{wj}$ represents the optimal bandwidth used for estimating the regression coefficient of the j-th explanatory variable, $\beta_{bwj}(u_i,v_i)$ represents the position $(u_i,v_i)$ corresponding to the regression coefficient of the $j$th variable, and $\epsilon_i$ is the error value of the normal distribution.

## Results and analysis

### Spatial distribution of soil erosion

In this study, the RUSLE model was employed to assess soil erosion in the CYUA. The validation of the model is provided in Supplementary Material S3. In this study, the RUSLE model was employed to evaluate soil erosion in the CYUA. From 1990 to 2020, notable spatial distribution characteristics of soil erosion in the CYUA were observed (Fig. 2). The data indicates that approximately 72.44% of the area did not exhibit significant soil erosion, while areas experiencing mild, moderate, and high-intensity erosion accounted for 16.69%, 7.04%, and 3.83%, respectively. It is noteworthy that from 1990 to 2000, the proportion of moderate and high-intensity erosion areas showed an increasing trend, peaking in 2020 at 9.42% and 7.75%, respectively. However, a reversal in trend occurred after 2000. By 2020, the proportions of moderate and high-intensity erosion areas decreased to 3.75% and 2.04%, respectively, representing a decrease of 151.13% and 182.16% compared to 2020, particularly evident in areas southwest near the Red River basin (Fig. 2a). The proportion of areas with no significant erosion exhibited an opposite trend, with the inflection point also occurring in 2000 (Fig. 2b).

### Identifying high-risk areas for soil erosion in CYUA

Using the improved Stability Mapping Method (STD), we classified the dynamic changes in soil erosion intensity levels in the Central Yunnan urban agglomeration from 1990 to 2020 into four primary categories: stable, stepwise, cyclical, and fluctuating, with further subdivisions into secondary and tertiary categories (Fig. 3). These categories reflect the changing characteristics of soil erosion across different regions and temporal scales.

The stable regions account for approximately 60.21% of the total area, primarily composed of persistently stable (49.97%) and long-term sustained (10.23%) types. This indicates that during the study period, most areas maintained a relatively stable soil erosion intensity with no significant changes, reflecting a stable ecological environment with minimal external disturbances. The stepwise regions comprise about 9.42% of the area, showing only one instance of change in soil erosion intensity, typically triggered by external disturbances during a specific phase (such as sudden rainfall or human activities), but subsequently returning to stability.Cyclical regions represent 16.70% of the total area and exhibit periodic fluctuations in soil erosion intensity. These areas are significantly influenced by seasonal or other periodic factors (such as rainfall or vegetation changes), indicating that soil erosion intensity follows a regular pattern over time.

Additionally, the fluctuating regions account for 13.68% of the area, characterized by frequent changes in soil erosion intensity, high turnover rates, and extreme instability. These areas are highly sensitive to changes in the external environment, such as precipitation intensity, vegetation cover, and variations in human activities, making them susceptible to soil degradation and heightened erosion risks. Therefore, in this study, fluctuating regions are identified as high-sensitivity zones for soil erosion, requiring focused attention and effective preventive measures.

Figure 3b illustrates the high-sensitivity areas are mostly distributed in northwestern Dayao County in the Chuxiong Prefecture, western Chuxiong City in the Chuxiong Prefecture, southern Gejiu City and Mengzi City in the Honghe Prefecture, as well as northeastern Huizei County and Xuanwei City in Qujing City, and eastern Luoping County in Qujing City. Combining this analysis with spatial distribution, we found a strong correlation between high-sensitivity areas for soil erosion and rivers rated above level five within the region. This suggests that areas along riverbanks may experience more severe soil erosion due to topographic variations and water flow erosion. This finding provides important reference data for soil and water conservation efforts in riverbank areas.

### Analysis of soil erosion driving factors

*Identification of dominant factors influencing soil erosion in the CYUA*

We selected 11 driving factors: elevation (X1), slope (X2), aspect (X3) topographic wetness index (X4), edge density (X5), landscape shape index (X6), major land use types (X7), population density(X8), vegetation coverage (X9), temperature (X10), and precipitation (X11). Utilizing the optimal parameters of the Optimal Parameter Geographical Detector, we quantitatively assessed the distribution of soil erosion in the CYUA over the past three decades. The results (Fig. 4) show that all 11 driving factors were statistically significant (sig < 0.05) and exhibited significant differences in their explanatory power for the soil erosion situation in the CYUA. Collectively, the q-value for slope (X2) was the highest ( $0.628\ ^{+0.051}_{-0.069}$), followed by vegetation coverage (X9) ( $0.531\ ^{+0.065}_{-0.084}$). This indicates these two factors mainly drive the spatial differentiation of soil erosion in the CYUA. Aspect (X3) showed the lowest explanatory power ( $0.205\ ^{+0.067}_{-0.069}$), while the other driving factors also had some influence on the spatial distribution of soil erosion, with their explanatory power fluctuating with time, with precipitation showing the most extensive fluctuation range in q-values ( $0.382\ ^{+0.085}_{-0.150}$).

The results of spatial detection (Fig. 5) indicate that, in most cases, the explanatory power of coupled factors exceeds that of single factors for soil erosion. Notably, the interaction between slope and precipitation and their

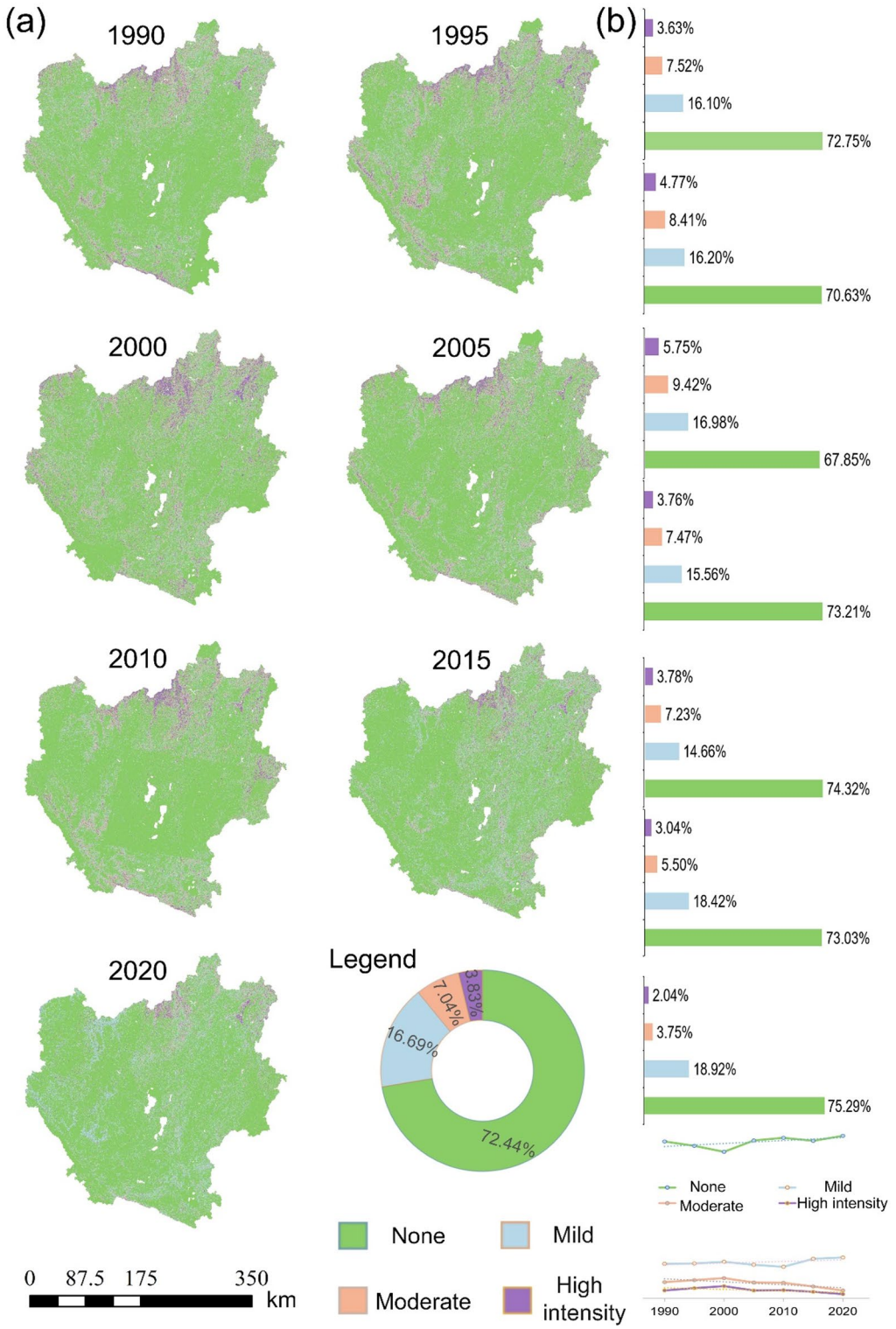


**Fig. 2**. Spatial-temporal distribution of soil erosion in the CYUA, where (**a**) illustrates the distribution of soil erosion intensity levels in the CYUA, and (**b**) depicts the proportion of soil erosion intensity at different periods and the trend of changes in intensity levels in the CYUA from 1990 to 2020. Figure 2 was generated though the ArcGIS 10.8 software (http://www.esri.com).

interactions with other factors demonstrate notably significant influences, with their combined explanatory power exceeding 0.6. Notably, the interaction between slope and precipitation stands out with an explanatory power as high as 0.97, nearly 2.54 times the explanatory power of rainfall as a single factor. Additionally, while vegetation coverage exhibits explanatory solid power as a standalone factor, its interaction with precipitation

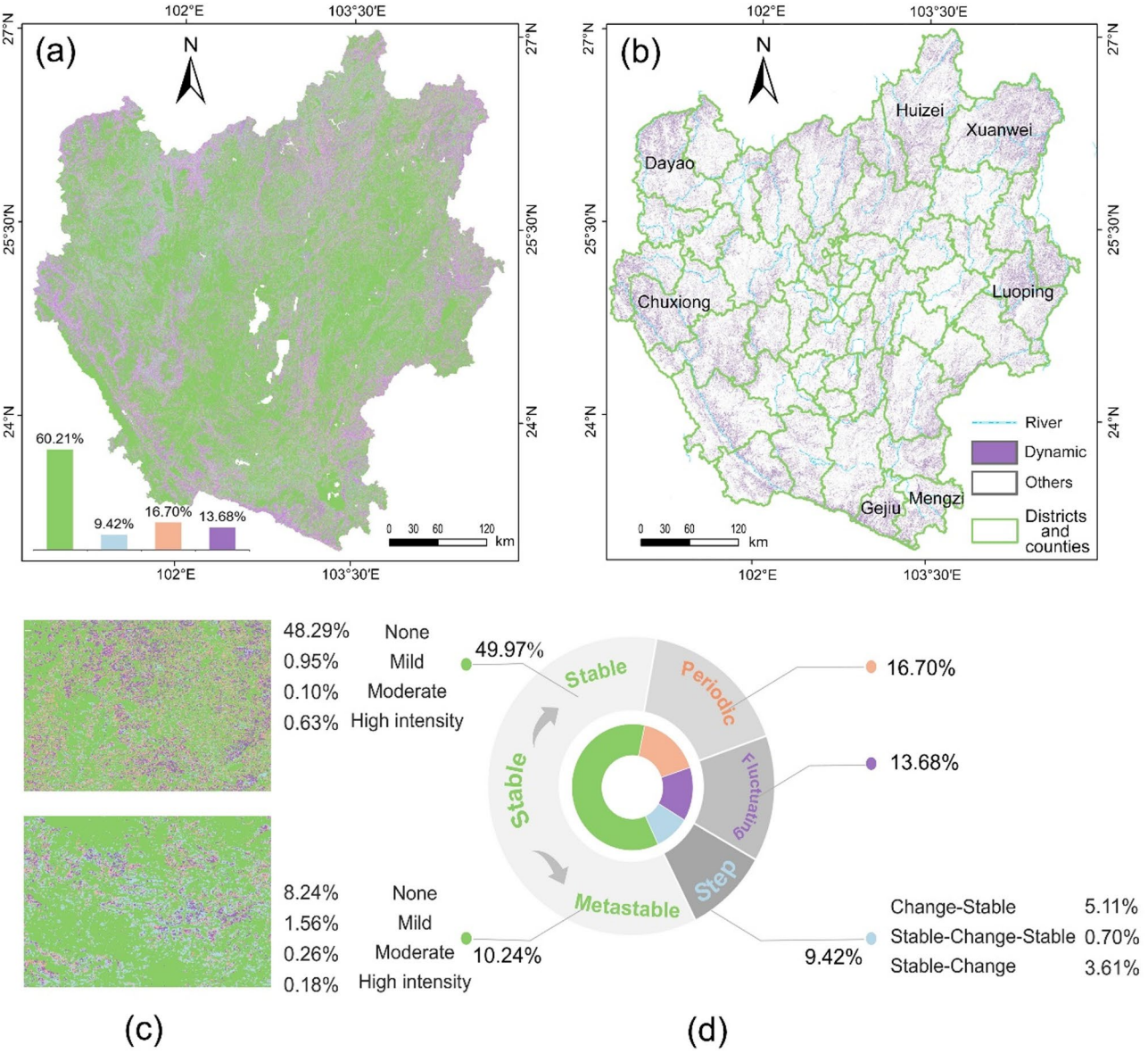


**Fig. 3**. Changes in STD trajectories of soil erosion in the CYUA from 1990 to 2020, where (**a**) illustrates the spatial distribution of soil erosion STD trajectory changes, (**b**) depicts the overlay of fluctuating areas of soil erosion in the CYUA with rivers of level five and above and districts (/counties), (**c**) presents a zoomed-in view of (**a**) (partial counties of Xundian and Mouding), and (**d**) shows the proportion of trajectory levels in STD trajectories. Figure 3 was generated though the ArcGIS 10.8 software (http://www.esri.com) and Microsoft PowerPoint (https://www.microsoft.com).

and population density further enhances its explanatory power, exceeding 0.7. These findings underscore the significant role of multifactor interactions in the spatial distribution of soil erosion, suggesting the importance of considering all potential interactive effects for a more accurate understanding and prediction of soil erosion spatial patterns.

The main drivers of soil erosion in the CYUA were identified as slope, vegetation coverage, and rainfall through the use of Optimal Parameter Geographical Detectors (OPGD) and Multiscale Geographically Weighted Regression (MGWR) methods. These factors were found to have significant spatial heterogeneity. The results (Table 4; Fig. 6) indicate that all driving factors passed the t-test ($P < 0.05$), demonstrating significant spatial heterogeneity. The slope exhibited firm spatial heterogeneity with a bandwidth of 45, positively correlated with soil erosion, with a mean regression coefficient of 0.832. This suggests that steeper slope areas experience more severe soil erosion issues, particularly in the northern and eastern regions of the CYUA. Vegetation coverage, with a bandwidth of 43, showed even more significant spatial heterogeneity, albeit with a lower correlation with soil erosion (mean regression coefficient of −0.448). However, its positive role in mitigating erosion must be considered, especially in areas with higher coverage along the northeast-to-southwest axis.

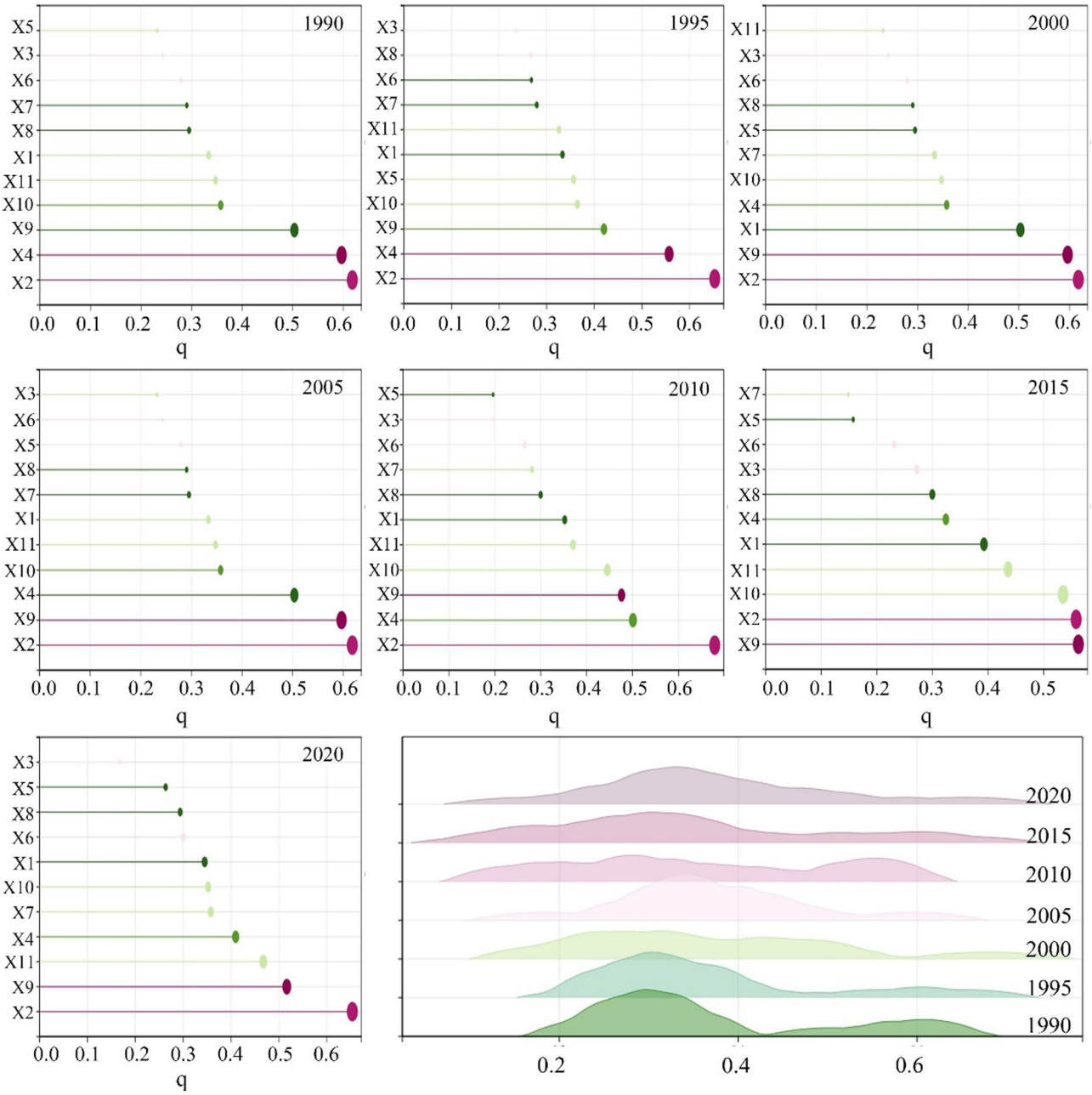


**Fig. 4**. Explanatory power of 11 driving factors on the spatial distribution of soil erosion in the CYUA. Figure 4 was generated though the SangerBox (http://www.Sangerbox.com).

*Identification of dominant factors in areas with high erosion-risk in the CYUA*

Areas with high erosion-risk in the CYUA from 1990 to 2020 were selected as the study objects, and factor detection was conducted for the 11 driving factors. The results (Fig. 7) indicate that eight factors passed the significance test. At the same time, the influences of elevation, aspect, and major land use types did not reach significance (with significance values greater than 0.05). Overall, rainfall (X11) exhibited the highest q-value ( $0.607\ ^{+0.099}_{-0.088}$), followed by vegetation coverage (X9) ( $0.524\ ^{+0.055}_{-0.099}$), highlighting these two as the main driving factors for high-risk soil erosion in the CYUA. Conversely, population density (X8) showed the weakest explanatory power ( $0.284\ ^{+0.039}_{-0.065}$). Additionally, other driving factors also influenced the spatial distribution of soil erosion in the CYUA, with their explanatory power fluctuating over time. Analysis of the q-values reveals slightly reduced single-factor explanatory power for high-intensity soil erosion compared to overall soil erosion in the CYUA. Nevertheless, single-factor explanatory power for high-intensity soil erosion displayed considerable fluctuation. Among numerous driving factors, the explanatory power of rainfall stands out, reaching its peak as a single factor, namely 0.705.


**Fig. 5**. Interaction explanatory power of 11 driving factors on soil erosion in the CYUA. Figure 5 was generated though the SangerBox (http://www.Sangerbox.com).

| Factor | Bandwidth | Mean | Minimum | Median | Maximum |
|---|---|---|---|---|---|
| Slope | 45 | 0.832 | 0.518 | 0.819 | 1.195 |
| FVC | 43 | −0.448 | −0.737 | −0.307 | −0.248 |
| Rainfall | 212 | 0.488 | 0.387 | 0.493 | 0.579 |

**Table 4**. Bandwidth and regression coefficients of key driving factors for overall soil Erosion in the MGWR model.

Interaction detection results (Fig. 8) indicate that any coupled two-factor interaction surpasses a single factor in explaining the spatial distribution high erosion-risk areas in the CYUA, with solid interaction explanatory powers exceeding 0.5. Notably, the interaction between terrain wetness index TWI (X4), a weak single-factor explanatory power, and temperature (X10) exhibits the highest interaction explanatory power for soil erosion in high-risk areas, reaching 0.91. The interaction between rainfall and vegetation coverage follows closely with an interaction explanatory power of 0.89. Additionally, the interaction between rainfall and slope demonstrates significant explanatory power, reaching 0.85.

The MGWR model reveals the impacts of three dominant driving factors (TWI, FVC, rainfall) on areas with high erosion-risk in the CYUA (Table 5; Fig. 9). Results indicate that the bandwidths of the three factors are larger than those of the entire region, with reduced spatial heterogeneity. TWI exhibits the most significant spatial heterogeneity with a bandwidth of 213, positively correlated with erosion (mean 0.258), particularly influencing

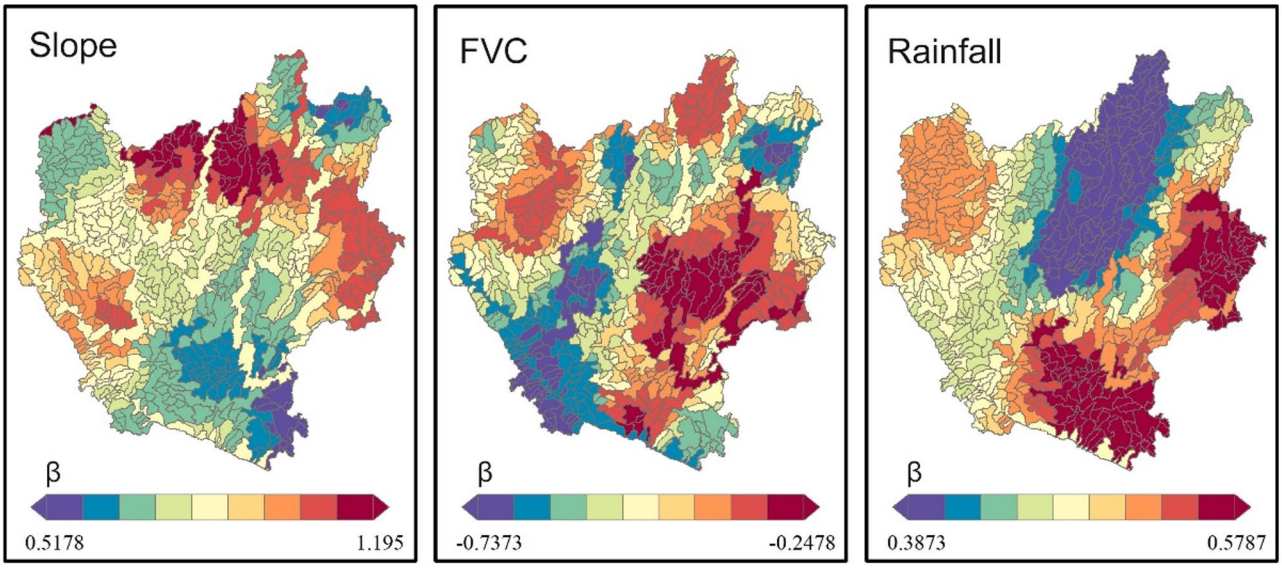


**Fig. 6**. Explicit spatial effects of slope, FVC, and rainfall on overall soil erosion in the CYUA through MGWR. Figure 6 was generated though the ArcGIS 10.8 software (http://www.esri.com).

the northern and southern areas. FVC, with a bandwidth of 547, shows less pronounced spatial heterogeneity, negatively correlated with erosion (mean −0.295), with notable inhibition observed in the southwest. Rainfall has the most considerable bandwidth (591) and the most significant positive promotion effect (mean 0.363), with high coefficient areas distributed in opposition to FVC, primarily in the north. Notably, areas with high rainfall coefficients exhibit an opposite trend to vegetation coverage factors, mainly distributed in the north.

## Discussion

### Innovation and generalizability of identifying high-risk areas based on the improved STD method

This study employed an improved Stability Mapping Method (STD) to identify high-risk areas for soil erosion, effectively overcoming the limitations of traditional methods that relied on single time-phase data and singular indicators[41]. Traditional approaches often focused solely on the intensity of soil erosion, whereas the improved STD method further incorporated temporal change characteristics, enabling a comprehensive assessment of the soil erosion process. Specifically, the improved STD method establishes a logically rigorous classification system by considering soil erosion similarity, turnover rate, and diversity. This system provides significant guidance for identifying different change types, allowing managers to quickly and accurately recognize and respond to soil erosion risks, thereby significantly enhancing decision-making efficiency and effectiveness.

Moreover, the STD method captures the complex dynamic changes of soil erosion processes, particularly in identifying fluctuating areas that are highly sensitive to environmental changes. This characteristic enhances the scientific accuracy of identifying high-sensitivity zones. The results show that areas with high erosion risk are primarily distributed along riverbanks, confirming the significant impact of water flow erosion on soil erosion[42]. This finding provides essential reference data for soil and water conservation efforts in riverbank areas, highlighting the need for relevant departments to strengthen vegetation protection and soil erosion control in these regions.

The improved STD method not only demonstrates significant advantages in soil erosion risk assessment but also possesses broad applicability through its multidimensional assessment framework. It can be extended to other ecologically sensitive fields. For example, assessing ecosystem degradation, biodiversity conservation, climate change impact assessment, land use change monitoring etc.

Importantly, identifying high-risk areas and implementing targeted management measures not only enhances the efficiency of ecological resource protection but also aligns with global sustainable development agendas[43], reinforcing the practical significance and social value of this research. In summary, the improved STD method provides a new perspective and tool for identifying and assessing various ecological issues by comprehensively considering temporal dimensions and changes across multiple indicators, with the potential for broader application in ecological environment management and protection, thereby enhancing the sustainable management capacity of ecosystems.

### Spatial heterogeneity of soil erosion driving mechanisms

This study employed an improved RUSLE model and STD stability mapping method to assess the temporal and spatial dynamic changes in soil erosion in the Central Yunnan urban agglomeration from 1990 to 2020. Additionally, OPGD and MGWR models were employed to reveal the differentiated driving mechanisms of soil

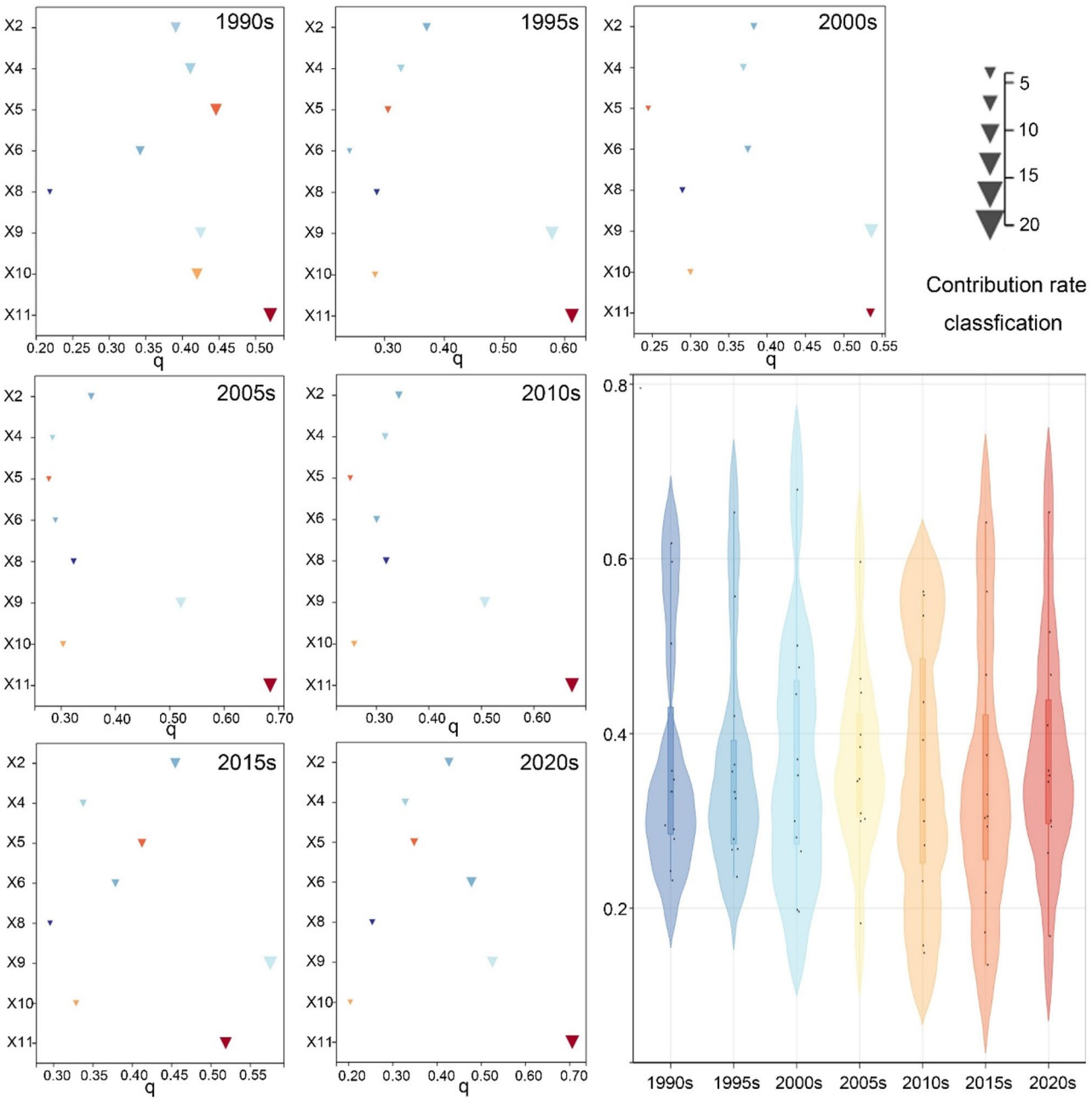


**Fig. 7**. Explanatory power of 8 driving factors on the spatial distribution of areas with high erosion-risk in the CYUA. Figure 7 was generated though the SangerBox (http://www.Sangerbox.com).

erosion in the urban agglomeration and high-risk erosion areas. This multi-model approach allowed for a more nuanced understanding of the complex interplay of factors influencing soil erosion at different spatial scales.

Initial Geographical detector analysis indicated that slope and vegetation cover were the primary factors influencing the spatial distribution of soil erosion across the Central Yunnan urban agglomeration. This aligned with previous research findings that terrain[44,45] and vegetation conditions[46] were key factors controlling regional soil erosion. This consistency across studies underscores the fundamental role of topography and land cover in shaping broad-scale erosion patterns. However, when focusing on high-risk erosion areas, the impact of precipitation and vegetation cover became more pronounced. This suggested that while topographic factors dominated at the regional scale, the influence of climatic conditions should not have been underestimated in local high-risk areas. This finding highlights a critical nuance: the dominant drivers of soil erosion can shift depending on the spatial scale of analysis. This underscored the importance of exploring internal regional differences to develop more targeted soil erosion control measures.

The application of the MGWR model provided further insights into the spatial heterogeneity characteristics of key driving factors, revealing nuances beyond the broad influence of slope and vegetation. Slope, vegetation

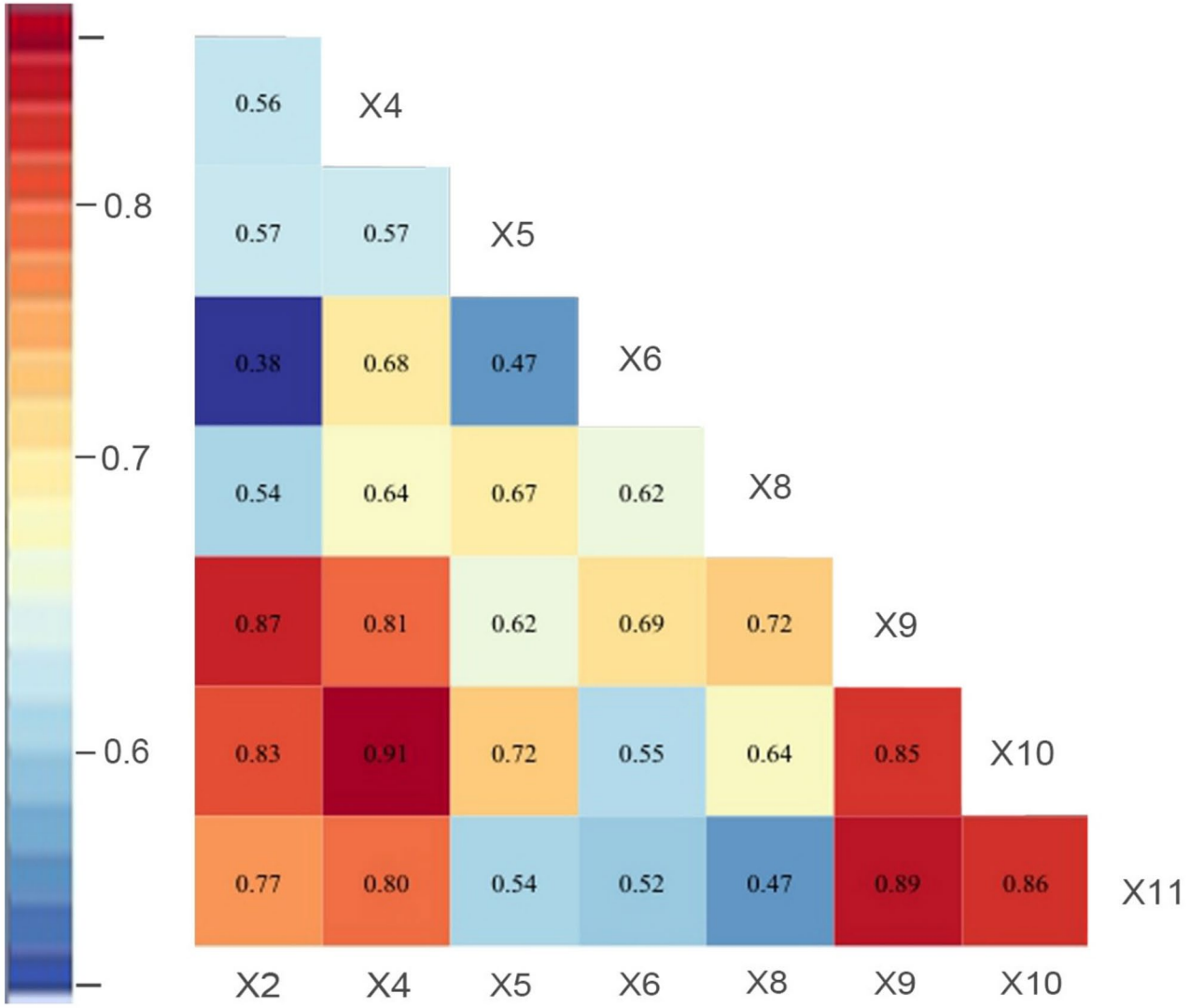


**Fig. 8**. Interaction explanatory power of 8 driving factors on areas with high erosion-risk in the CYUA. Figure 8 was generated though the SangerBox (http://www.Sangerbox.com).

| Factor | Bandwidth | Mean | Minimum | Median | Maximum |
|---|---|---|---|---|---|
| TWI | 213 | 0.258 | 0.056 | 0.246 | 0.583 |
| FVC | 547 | −0.295 | −0.405 | −0.307 | −0.191 |
| Rainfall | 591 | 0.363 | 0.274 | 0.366 | 0.583 |

**Table 5**. Bandwidth and regression coefficients of key driving factors for areas with high Erosion risk in the MGWR.

cover, and precipitation exhibited distinct spatial impact patterns. Slope primarily affected the northern and eastern regions of the urban agglomeration, suggesting its dominant role in areas with steeper terrain. The influence of vegetation cover was more significant along the northeast to southwest axis, potentially reflecting the distribution of different vegetation types and their effectiveness in erosion control. Notably, precipitation had the largest impact scale, showing a more apparent positive correlation with soil erosion in high rainfall areas. These spatially varying relationships emphasize the importance of considering local environmental conditions when assessing erosion risk. These results highlight significant differences in the spatial effects of various factors, likely stemming from the inherent spatial variations in terrain, climate, and vegetation conditions within the region. Therefore, formulating effective soil erosion control strategies necessitates considering the spatial heterogeneity of key factors and implementing water and soil conservation efforts tailored to local conditions.

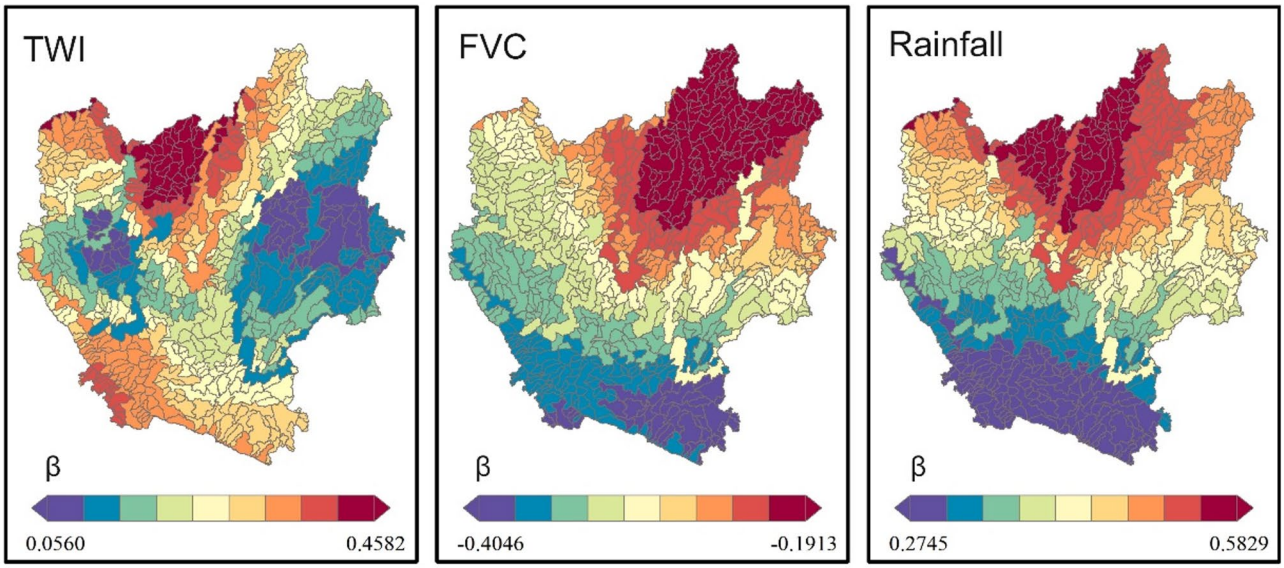


**Fig. 9**. Spatially explicit effects of MGWR, TWI, FVC, and rainfall on areas with high erosion-risk of the CYUA. Figure 9 was generated though the ArcGIS 10.8 software (http://www.esri.com).

Furthermore, MGWR analysis results for high erosion risk areas revealed that the topographic wetness index (TWI), along with vegetation cover and precipitation, emerged as dominant factors. Interestingly, the spatial heterogeneity of these factors was reduced compared to the overall region. This may be attributed to the relatively consistent environmental conditions within these high-risk areas, leading to diminished spatial variability in driving factors. Nonetheless, TWI, vegetation cover, and precipitation still exhibited noticeable spatial differentiation at the local scale. The topographic wetness index had a greater influence in the northern and southern areas, indicating its importance in areas prone to water accumulation. Conversely, vegetation cover had a more pronounced suppressive effect in the southwestern region. This suggests that even within high-risk zones, specific localized factors can modulate erosion processes, requiring fine-tuned interventions. These findings emphasize the necessity of exploring internal regional differences even within high-risk zones, providing important references for precise policy-making and targeted interventions.

## Significant mitigating effect of vegetation on soil erosion: unpacking the mechanisms

Our research consistently indicated that vegetation cover significantly mitigates soil erosion, both across the entire study area and within high erosion risk zones. This strong negative correlation aligns with numerous studies demonstrating the protective role of vegetation[15,47]. Our findings further elucidate the underlying mechanisms: First, the roots of vegetation penetrate deep into the soil, effectively increasing soil stability and reducing the risk of excessive runoff[48], thereby alleviating soil erosion. Second, the presence of vegetation acts as a physical barrier, slowing down water flow and reducing its erosive power, thus decreasing the scouring effect of water on the soil and enhancing soil resistance to erosion[49]. Additionally, vegetation significantly improves rainfall interception capacity[50], reducing the amount of rainfall directly impacting the soil surface. Furthermore, vegetation enhances soil water retention, which not only helps protect soil structure but also effectively prevents soil and water loss.

Moreover, MGWR analysis results further validate the significant negative correlation between vegetation cover and soil erosion, clearly indicating that increasing vegetation cover is a highly effective soil and water conservation strategy[15]. This reinforces the established understanding of vegetation as a key tool for erosion control. By comparing data from 1990 to 2020, we observed that the severe soil erosion conditions in the southwestern region of the Central Yunnan urban agglomeration improved, a change directly attributable to increased vegetation cover. This temporal observation provides empirical evidence supporting the long-term effectiveness of vegetation restoration efforts in reducing erosion. This finding emphasizes the critical and multifaceted role of vegetation in preventing soil erosion, particularly in high-intensity erosion scenarios[47]. Therefore, in future soil erosion control efforts, especially in vulnerable areas like the downstream Jinsha River and upstream Nanpan River, which are significantly affected by rainfall, it is essential to prioritize the protection and restoration of vegetation to effectively prevent soil erosion and safeguard regional ecological safety[51].

## Research limitations

This study investigated the spatio-temporal variations and the mechanisms driving soil erosion in the CYUA over the past thirty years, yielding some important findings. However, some limitations and uncertainties were still worthy of further analysis and discussion. First, we did not finely classify the specific values of key driving factors, unable to accurately capture the subtle distinctions in soil erosion under differing levels of factors. Future research could supplement this by delving deeper to reveal the differential effects of diverse factors on soil erosion.

Second, we analyzed the driving forces of soil erosion separately at the grid scale (OPGD) and the basin scale (MGWR). However, soil erosion processes differed across scales due to hydrological conditions' nonlinearity, heterogeneity, and randomness[37,52]. Future research could conduct multiscale analyzes to understand soil erosion processes comprehensively[53,54]. Despite these limitations, this study provided new insights and methods for soil erosion management in the CYUA. The research outcomes provided a scientific basis for formulating more targeted and actionable soil protection measures.

## Conclusion

This study assessed the temporal and spatial dynamic changes in soil erosion in the Central Yunnan urban agglomeration from 1990 to 2020 based on an improved RUSLE model and the STD stability mapping method. Additionally, OPGD and MGWR models were utilized to reveal the differentiated driving mechanisms of soil erosion in the overall urban agglomeration and high-risk erosion areas. The main conclusions are as follows:

(1) From 1990 to 2020, soil erosion in the Central Yunnan urban agglomeration exhibited a trend of first intensifying and then alleviating, with inflection points for moderate and high-intensity erosion areas occurring in 2000.
(2) Using the improved STD method, high-risk soil erosion areas were identified mainly along the riverbanks of the urban agglomeration, which are highly sensitive to external disturbances and require enhanced soil and water conservation measures.
(3) OPGD analysis indicated that slope and vegetation are key factors influencing the overall soil erosion patterns of the urban agglomeration, while precipitation and vegetation are the dominant influencing factors in high-risk areas. Significant interactive effects exist among different factors.
(4) The MGWR model revealed the spatial heterogeneity characteristics of key driving factors. Slope primarily affects the northern and eastern regions, while vegetation has a significant role along the northeast-southwest axis, and precipitation has the largest impact scale. The spatial heterogeneity of driving factors in high-risk areas is reduced compared to the overall region.
(5) The mitigating effect of vegetation cover on soil erosion is significant. Increasing vegetation cover is an effective soil and water conservation strategy, and future efforts should focus on the protection and restoration of vegetation in the northern region of the Jinsha River and the upper reaches of the Nanpan River.

## Data availability

All data generated or analyzed during this study are included in this published article. For any inquiries, please reach out to the corresponding author.

Received: 8 November 2024; Accepted: 6 May 2025
Published online: 15 May 2025

## References

1. Amundson, R. et al. Soil and human security in the 21st century. *Science* **348**, 1261071. https://doi.org/10.1126/science.1261071 (2015).
2. Stocking, M. A. Tropical soils and food security: the next 50 years. *Science* **302**, 1356–1359. https://doi.org/10.1126/science.1088579 (2003).
3. Skaalsveen, K., Ingram, J. & Clarke, L. E. The effect of no-till farming on the soil functions of water purification and retention in north-western Europe: A literature review. *Soil Tillage. Res.* **189**, 98–109. https://doi.org/10.1016/j.still.2019.01.004 (2019).
4. Dance, A. Soil ecology: what Lies beneath. *Nature* **455**, 724–725. https://doi.org/10.1038/455724a (2008).
5. Sonderegger, T. & Pfister, S. Global assessment of agricultural productivity losses from soil compaction and water Erosion. *Environ. Sci. Technol.* **55**, 12162–12171. https://doi.org/10.1021/acs.est.1c03774 (2021).
6. Montanarella, L. et al. World's soils are under threat. *SOIL* **2**, 79–82. https://doi.org/10.5194/soil-2-79-2016 (2016).
7. Brown, L. R. World population growth, soil erosion, and food security. *Science* **214**, 995–1002. https://doi.org/10.1126/science.7302578 (1981).
8. Tang, X. et al. Soil C, N, P stocks and stoichiometry as related to land use types and erosion conditions in lateritic red soil region, South China. *CATENA* **210**, 105888. https://doi.org/10.1016/j.catena.2021.105888 (2022).
9. Leng, S. et al. Key research areas and problems of soil erosion and soil conservation science. *J. Soil Water Conserv.* **1**, 1–6 (2004).
10. Borrelli, P. et al. An assessment of the global impact of 21st century land use change on soil erosion. *Nature Communications* 8, (2013). (2017) https://doi.org/10.1038/s41467-017-02142-7
11. Wen, B. et al. Spatiotemporal dynamics and driving factors of soil erosion in the Beiluo river basin, loess plateau, China. *Ecol. Ind.* **155**, 110976. https://doi.org/10.1016/j.ecolind.2023.110976 (2023).
12. Cao, Y., Hua, L., Tang, Q., Liu, L. & Cai, C. Evaluation of monthly-scale soil erosion spatio-temporal dynamics and identification of their driving factors in Northeast China. *Ecol. Ind.* **150**, 110187. https://doi.org/10.1016/j.ecolind.2023.110187 (2023).
13. Liang, S. & Fang, H. Quantitative analysis of driving factors in soil erosion using geographic detectors in qiantang river catchment, Southeast China. *J. Soils Sediments*. **21**, 134–147. https://doi.org/10.1007/s11368-020-02756-3 (2021).
14. Yang, Y. & Song, G. Human disturbance changes based on Spatiotemporal heterogeneity of regional ecological vulnerability: A case study of Qiqihaer City, Northwestern Songnen plain, China. *J. Clean. Prod.* **291**, 125262. https://doi.org/10.1016/j.jclepro.2020.125262 (2021).
15. Ma, T. et al. Response of soil erosion to vegetation and terrace changes in a small watershed on the loess plateau over the past 85 years. *Geoderma* **443**, 116837. https://doi.org/10.1016/j.geoderma.2024.116837 (2024).
16. Wang, Y. et al. Spatiotemporal characteristics and driving mechanisms of land use/land cover (LULC) changes in the Jinghe river basin, China. *J. Arid Land.* **16**, 91–109. https://doi.org/10.1007/s40333-024-0051-x (2024).
17. Daryanto, S., Wang, L. & Jacinthe, P. A. No-till is challenged: complementary management is crucial to improve its environmental benefits under a changing climate. *Geogr. Sustain.* **1**, 229–232. https://doi.org/10.1016/j.geosus.2020.09.003 (2020).
18. Borrelli, P. et al. Land use and climate change impacts on global soil erosion by water (2015–2070). *Proceedings of the National Academy of Sciences* 117, 21994–22001 (2020). https://doi.org/10.1073/pnas.2001403117
19. Guo, Y. et al. Modelling the impacts of climate and land use changes on soil water erosion: model applications, limitations and future challenges. *J. Environ. Manage.* **250**, 109403. https://doi.org/10.1016/j.jenvman.2019.109403 (2019).

20. Polykretis, C., Grillakis, M. G., Manoudakis, S., Seiradakis, K. D. & Alexakis, D. D. Spatial variability of water-induced soil erosion under climate change and land use/cover dynamics: from assessing the past to foreseeing the future in the mediterranean Island of Crete. *Geomorphology* **439**, 108859. https://doi.org/10.1016/j.geomorph.2023.108859 (2023).
21. Zhang, Y. et al. Dynamic analysis of soil erosion in the affected area of the lower yellow river based on RUSLE model. *Heliyon* **10** https://doi.org/10.1016/j.heliyon.2023.e23819 (2024).
22. Wei, B., Li, Z., Duan, L., Gu, Z. & Liu, X. Vegetation types and rainfall regimes impact on surface runoff and soil erosion over 10 years in karst hillslopes. *CATENA* **232**, 107443. https://doi.org/10.1016/j.catena.2023.107443 (2023).
23. Nauman, T. W., Munson, S. M., Dhital, S., Webb, N. P. & Duniway, M. C. Synergistic soil, land use, and climate influences on wind erosion on the Colorado plateau: implications for management. *Sci. Total Environ.* **893**, 164605. https://doi.org/10.1016/j.scitotenv.2023.164605 (2023).
24. Hao, R. et al. Impacts of changes in climate and landscape pattern on ecosystem services. *Sci. Total Environ.* **579**, 718–728. https://doi.org/10.1016/j.scitotenv.2016.11.036 (2017). https://doi.org/https://doi.org/
25. Feng, Q., Zhao, W., Fu, B., Ding, J. & Wang, S. Ecosystem service trade-offs and their influencing factors: A case study in the loess plateau of China. *Sci. Total Environ.* **607–608**, 1250–1263. https://doi.org/10.1016/j.scitotenv.2017.07.079 (2017).
26. Li, Y., Ma, J., Xiao, C. & Li, Y. Effects of climate factors and soil properties on soil nutrients and elemental stoichiometry across the Huang–Huai–Hai river basin, China. *J. Soils Sediments.* **20**, 1970–1982. https://doi.org/10.1007/s11368-020-02583-6 (2020).
27. Wang, K. et al. Impacts of vegetation restoration on soil erosion in the yellow river basin, China. *CATENA* **234**, 107547. https://doi.org/10.1016/j.catena.2023.107547 (2024).
28. Liu, W. et al. Spatio-temporal variations of ecosystem services and their drivers in the Pearl river delta, China. *J. Clean. Prod.* **337**, 130466. https://doi.org/10.1016/j.jclepro.2022.130466 (2022).
29. Pribadi, D. O. & Pauleit, S. Peri-urban agriculture in Jabodetabek metropolitan area and its relationship with the urban socioeconomic system. *Land. Use Policy.* **55**, 265–274. https://doi.org/10.1016/j.landusepol.2016.04.008 (2016).
30. Ju, H. et al. Driving forces and their interactions of built-up land expansion based on the geographical detector – a case study of Beijing, China. *Int. J. Geogr. Inf. Sci.* **30**, 2188–2207. https://doi.org/10.1080/13658816.2016.1165228 (2016).
31. Lu, R., Dai, E. & Wu, C. Spatial and Temporal evolution characteristics and driving factors of soil conservation services on the Qinghai-Tibet plateau. *CATENA* **221**, 106766. https://doi.org/10.1016/j.catena.2022.106766 (2023).
32. Ranstam, J. & Cook, J. A. LASSO regression. *Br. J. Surg.* **105**, 1348–1348. https://doi.org/10.1002/bjs.10895 (2018).
33. Song, Y., Wang, J., Ge, Y. & Xu, C. An optimal parameters-based geographical detector model enhances geographic characteristics of explanatory variables for Spatial heterogeneity analysis: cases with different types of Spatial data. *GIScience Remote Sens.* **57**, 593–610. https://doi.org/10.1080/15481603.2020.1760434 (2020).
34. Guo, B., Yang, F., Fan, Y. & Zang, W. The dominant driving factors of Rocky desertification and their variations in typical mountainous karst areas of Southwest China in the context of global change. *CATENA* **220**, 106674. https://doi.org/10.1016/j.catena.2022.106674 (2023).
35. Ganasri, B. P. & Ramesh, H. Assessment of soil erosion by RUSLE model using remote sensing and GIS - A case study of Nethravathi basin. *Geosci. Front.* **7**, 953–961. https://doi.org/10.1016/j.gsf.2015.10.007 (2016).
36. Tang, Q., Xu, Y., Bennett, S. J. & Li, Y. Assessment of soil erosion using RUSLE and GIS: a case study of the Yangou watershed in the loess plateau, China. *Environ. Earth Sci.* **73**, 1715–1724. https://doi.org/10.1007/s12665-014-3523-z (2015).
37. Shi, P., Chen, J. & Pan, Y. Analysis of land use change mechanism in Shenzhen. *Acta Geogr. Sin.* **55**, 151–160 (2000).
38. Swetnam, R. D. Rural land use in England and Wales between 1930 and 1998: mapping trajectories of change with a high resolution spatio-temporal dataset. *Landsc. Urban Plann.* **81**, 91–103. https://doi.org/10.1016/j.landurbplan.2006.10.013 (2007).
39. Fotheringham, A. S., Yang, W. & Kang, W. Multiscale geographically weighted regression (MGWR). *Annals Am. Association Geographers.* **107**, 1247–1265. https://doi.org/10.1080/24694452.2017.1352480 (2017).
40. Hu, J., Zhang, J. & Li, Y. Exploring the Spatial and Temporal driving mechanisms of landscape patterns on habitat quality in a City undergoing rapid urbanization based on GTWR and MGWR: the case of Nanjing, China. *Ecol. Ind.* **143**, 109333. https://doi.org/10.1016/j.ecolind.2022.109333 (2022).
41. Li, S., Xiao, W., Zhao, Y. & Lv, X. Incorporating ecological risk index in the multi-process MCRE model to optimize the ecological security pattern in a semi-arid area with intensive coal mining: A case study in Northern China. *J. Clean. Prod.* **247**, 119143. https://doi.org/10.1016/j.jclepro.2019.119143 (2020).
42. Negese, A. Impacts of land use and land cover change on soil erosion and hydrological responses in Ethiopia. *Appl. Environ. Soil. Sci.* **6669438** 2021 (2021).
43. Colglazier, W. Sustainable development agenda: 2030. *Science* **349**, 1048–1050. https://doi.org/10.1126/science.aad2333 (2015).
44. Benaud, P. et al. National-scale geodata describe widespread accelerated soil erosion. *Geoderma* **371**, 114378. https://doi.org/10.1016/j.geoderma.2020.114378 (2020).
45. Duan, X. et al. Investigation method for regional soil erosion based on the Chinese soil loss equation and high-resolution Spatial data: case study on the mountainous Yunnan Province, China. *CATENA* **184**, 104237. https://doi.org/10.1016/j.catena.2019.104237 (2020).
46. Liu, Z. Y., Zhang, J., Wang, J., TEMPORAL AND SPATIAL VARIATION OF SOIL & EROSION IN CENTRAL YUNNAN PROVINCE. *CHINA Appl. Ecol. Environ. Res.* **18**, 6691–6712 https://doi.org/10.15666/aeer/1805_66916712 (2020).
47. Wang, L., Cherkauer, K. A. & Flanagan, D. C. Impacts of Climate Change on Soil Erosion in the Great Lakes Region. *Water* 10 (2018).
48. Vannoppen, W., Vanmaercke, M., De Baets, S. & Poesen, J. A review of the mechanical effects of plant roots on concentrated flow erosion rates. *Earth Sci. Rev.* **150**, 666–678. https://doi.org/10.1016/j.earscirev.2015.08.011 (2015).
49. Mohammad, A. G. & Adam, M. A. The impact of vegetative cover type on runoff and soil erosion under different land uses. *CATENA* **81**, 97–103. https://doi.org/10.1016/j.catena.2010.01.008 (2010).
50. Sastre, B., Barbero-Sierra, C., Bienes, R., Marques, M. J. & García-Díaz, A. Soil loss in an Olive grove in central Spain under cover crops and tillage treatments, and farmer perceptions. *J. Soils Sediments.* **17**, 873–888. https://doi.org/10.1007/s11368-016-1589-9 (2017).
51. Rao, W., Shen, Z. & Duan, X. Spatiotemporal patterns and drivers of soil erosion in Yunnan, Southwest China: RULSE assessments for recent 30 years and future predictions based on CMIP6. *CATENA* **220**, 106703. https://doi.org/10.1016/j.catena.2022.106703 (2023).
52. Shengdong, C., Penglei, H., Zhaohong, F., Zhanbin, L. & Tiegang, Z. Fractal characters of soil erosion Spatial pattern in the watershed on loess plateau, China. *Nat. Environ. Pollution Technol.* **17**, 1359–1366 (2018).
53. Kaiser, A., Erhardt, A. & Eltner, A. Addressing uncertainties in interpreting soil surface changes by multitemporal high-resolution topography data across scales. *Land. Degrad. Dev.* **29**, 2264–2277 (2018).
54. Gao, G., Fu, B., Zhang, J., Ma, Y. & Sivapalan, M. Multiscale Temporal variability of flow-sediment relationships during the 1950s–2014 in the loess plateau, China. *J. Hydrol.* **563**, 609–619. https://doi.org/10.1016/j.jhydrol.2018.06.044 (2018).


## Acknowledgements

This work was supported by the National Natural Science Foundation of China(42261073, 41971369, 42261037), Yunnan Province Reserve Talent Program for Young and Middle-aged Academic and Technical Leaders (202305 AC160083、202205 AC160014), Major Scientific and Technological Projects of Yunnan Province

(202202 AD080010),Yunnan Provincial Basic Research Project (202401 AT070103, 202201 AS070024, 202001 AS070032).

## Author contributions

Dongling Ma, Data curation, Methodology, Validation, Visualization, Formal analysis, Writing – original draft. Shuangyun Peng, Conceptualization, Supervision, Resources, Funding acquisition, Writing – review & editing. Zhiqiang Lin, Methodology, Investigation, Writing – review & editing. Bangmei Huang, Resources. Ziyi Zhu: Formal analysis, Shuangfu Shi, Supervision.

## Declarations

## Competing interests

The authors declare no competing interests.

## Additional information

**Supplementary Information** The online version contains supplementary material available at https://doi.org/10.1038/s41598-025-01443-y.

**Correspondence** and requests for materials should be addressed to S.P.

**Reprints and permissions information** is available at www.nature.com/reprints.

**Publisher's note** Springer Nature remains neutral with regard to jurisdictional claims in published maps and institutional affiliations.